ELSEVIER

0266-8920(95)00018-6

Probabilistic Engineering Mechanics **10** (1995) 225–240

0266-8920/95/$09.50

Surge response statistics of tension leg platforms under wind and wave loads: a statistical quadratization approach

Ahsan Kareem

Department of Civil Engineering & Geological Sciences, University of Notre Dame, Notre Dame, IN 46556-0767, U.S.A.

Jun Zhao

Barnett & Casbarian, Inc., Houston, TX 77024-1596, U.S.A.

&

Michael A. Tognarelli

Department of Civil Engineering & Geological Sciences, University of Notre Dame, Notre Dame, IN 46556-0767, U.S.A.

Commonly, in offshore applications, frequency domain analyses of nonlinear systems have been approximately carried out using the method of equivalent statistical linearization. This method, however, fails to capture the non-Gaussianity of the response in terms of its higher-order statistics. In addition, response energy in frequency ranges outside that of the input spectrum is not observed using this technique. Herein, a method of equivalent statistical quadratization is proposed, whereby a statistically asymmetric nonlinearity in the forcing of a tension leg platform (TLP) is cast in a quadratic form. The present quadratization method takes advantage of the Gaussianity of the first order response to simplify the recasting of the nonlinearity in its approximate polynomial form. A Volterra series approach leads to the development of transfer functions from which the response spectrum as well as statistics of the response may be obtained. Response cumulants, computed up to fourth order via direct integration or the Kac–Siegert technique, reveal the non-Gaussian character of the response which was hidden by linearization and, when used in the framework of some available non-Gaussian probability density function models, indicate acceptable agreement with time-domain simulations of the original nonlinear differential equations. In addition, the response power spectral density contains an additional peak near the resonant frequency of the TLP, where input energy at difference frequencies of the input spectrum lies, corroborating information gleaned from the time-domain simulation.

INTRODUCTION

The challenge of developing deep water oil fields has placed a growing importance on the economics and safety issues concerning drilling and production platforms. The tension leg platform (TLP) is the most promising structural concept among different structural systems being considered for deep water applications. The compliant nature of TLP motions in the horizontal plane makes these platforms sensitive to low frequency oscillations due to wind and wave drift forces. Both the wind loads and wave loads acting on TLPs are nonlinear, for example, wind loading in the presence of the square of the fluctuating velocity term and the wave drag force in the Morison equation[1] which contains a nonlinear term involving the water particle velocity. Furthermore, the hydrodynamic loads due to potential effects (diffraction and radiation) contain inherent quadratic load effects (e.g. Refs 1 and 2). Historically, analyses of nonlinear systems in the frequency domain have been based on the statistical linearization approach (e.g. Refs 3–5). The linearization approach, however, fails to adequately represent important features of the nonlinearity. Particularly, the response power spectral density function spans only the range of excitation frequencies while the energy at the sum and difference frequency components is nonexistent. Further, the response probability density function remains Gaussian, giving rise to underprediction of the response extremes which are very important for design considerations.

The concept of quadratization or polynomial approximation of nonlinear effects has been used in the study of hydrodynamic loads on offshore structures (e.g. Refs 6–20). Most of these studies are limited to obtaining the second-order statistics of the loading or response process while some are extended to extremes of wave force statistics and higher-order response cumulants. Spanos and Donley[13–15] formulated a more general quadratization technique for the treatment of arbitrarily statistically asymmetric nonlinear systems. The investigation established frequency domain moment expressions up to the third order, but considered fourth-order moment computations prohibitive, and developed a probability density function estimation based on the Gram–Charlier expansion. Kareem and Zhao[17–19] formulated an alternative quadratization method for the analysis of nonlinear wind and wave loads on TLPs which capitalized, in terms of computational efficiency, on the Gaussianity of the first-order response solution. An integral factorization developed in their studies helped to make calculations of fourth-order response statistics feasible, and more accurate probability density approximations possible. References 17, 18 and 20 also investigate a procedure termed equivalent statistical cubicization for use in cases when the nonlinearity is statistically symmetric. This paper addresses the response of a TLP to wind and wave loads. The nonlinear loading is expressed via quadratization in terms of an equivalent polynomial that contains terms up to quadratic order.

THEORETICAL BACKGROUND

Historically, two fundamental approaches exist for solving nonlinear stochastic problems: one rooted in the theory of Markov processes and the associated Fokker–Planck equation, and the other based on frequency domain analysis. Herein, we will pursue the latter approach by assimilating a nonlinear system to a quadratic form utilizing the method of equivalent statistical quadratization and applying the Volterra theory for system analysis in the frequency domain. Thereby, we will be able to establish statistical descriptors for the system response up to fourth-order to more accurately characterize its non-Gaussian nature. The statistical quantities thus obtained may be employed within several current frameworks for estimating probability distributions and crossing rates of non-Gaussian processes, with the ultimate goal of effectively describing the extremes of the response process.

Volterra series

A Volterra series expansion may be viewed as a regular expansion in power series, 'with memory'.[21] We may treat the system with a polynomial nonlinear transformation as a Volterra equivalent system. The general second-order Volterra equivalent system may be described as the following,

$$x(t) = \int_{-\infty}^{\infty} h_1(\tau)u(t-\tau)\,\mathrm{d}\tau + \frac{1}{2}\int_{-\infty}^{\infty}\int h_2(\tau,\sigma) \times u(t-\tau)u(t-\sigma)\,\mathrm{d}\tau\,\mathrm{d}\sigma = x_1(t) + \tfrac{1}{2}x_2(t) \quad (1)$$

where $u(t)$ is an input process, $h_1(\tau)$ and $h_2(\tau,\sigma)$ are linear and second-order impulse response functions, respectively, and $x_1(t)$ and $x_2(t)$ are linear and second-order response components. Notice that the first-order kernel is simply the impulse response function of a linear system, while the higher-order kernels can be viewed as higher-order impulse response functions which serve to characterize the various orders of nonlinearities. The general formulation of the kernels is not available, but when the nonlinear transformation is in the polynomial form, the kernels can be evaluated. The application of this series to nonlinear systems was first investigated by Wiener[24] in 1942. Later, Barrett[25] reported on a systematic study of the utility of the Volterra series for analyzing physical systems.

The first term of eqn (1), representing the output of a first-order Volterra system, is the same as the response of a linear, time-invariant system. The second term in (1) is a two-dimensional convolution which represents the output of a second-order Volterra system where $h_2(\tau,\sigma)$ is the second-order Volterra kernel and is generally assumed symmetric. This kernel is related to the quadratic transfer function by,

$$H_2(\omega_1,\omega_2) = \int_{-\infty}^{\infty}\int_{-\infty}^{\infty} h_2(\tau_1,\tau_2)\,\mathrm{e}^{-i\omega_1\tau_1}\,\mathrm{e}^{-i\omega_2\tau_2}\,\mathrm{d}\tau_1\,\mathrm{d}\tau_2. \quad (2)$$

Clearly, then, the response of the second-order Volterra system will contain energy at frequencies which are, in fact, the sums and differences of frequencies contained in the input.

Types of nonlinearities

In this study we will cast a nonlinear system in the form of the Volterra functional series up to the second order for the purpose of statistical analysis. It is first important to note that the statistical characteristics of a given nonlinearity make it more or less conducive to analysis by a particular order Volterra system. Indeed, a *statistically symmetric* nonlinear function, $g(u)$, defined as a function for which $E[g(u)^{2n-1}] = 0$ for all n, is not treatable by the quadratization technique. Conversely, a *statistically asymmetric* nonlinear function, $g(u)$, for which $E[g(u)^{2n-1}]$ is nonzero for all n, may be effectively approximated by the present technique. Given a zero-mean, Gaussian process, $u(t)$, the functions $g(u) = (u+a)\,|u+a|$ and $g(u) = u^2$ are examples of statistically asymmetric nonlinearities.[17]

Modeling of wind and wave loads

The compliant nature of TLP motions in the horizontal plane makes their surge response sensitive to wind-induced drag force fluctuations. Some works covering the second-order statistical characterization of the response of a TLP under the dynamic effects of wind are found in Refs 11 and 27–31. Kareem and Zhao[19] developed the analysis to include up to fourth-order response statistics using an equivalent statistical quadratization technique as well as the Kac–Siegert approach. For more detail on the modeling of wind loads, the reader is referred to Ref. 32.

Typical TLP structures, depending on their submerged geometry and size, experience a combination of wave-induced viscous and potential loads. The viscous effects are generally described through the drag term of the Morison equation, for example,

$$F_u(t,\dot{x}) = \int_{S_v} 0{\cdot}5\rho C_d\,|u(y,z,t) - \dot{x}(t)|\times(u(y,z,t) - \dot{x}(t))\,\mathrm{d}s, \quad (3)$$

where $F_u(t,\dot{x})$ is the viscous force, S_v is the submerged surface area, ρ and C_d are water density and a force coefficient, respectively, and u is the water particle velocity. The first-order diffraction loads are given by the convolution of the wave surface elevation, $\eta(t)$, with an appropriate convolution kernel. The wave radiation force is given in terms of frequency-dependent added mass and radiation coefficients which can be obtained from diffraction analysis.

The higher-order effects resulting from hydrodynamic loads of viscous and potential origins introduce nonlinearity with the consequence of non-Gaussian statistical features. These higher-order effects are attributable to the following sources: (i) nonlinearity in Bernoulli's equation; (ii) nonlinearity in the Morison drag term; (iii) nonlinearity in the free surface wave profile; (iv) displacement and velocity dependence of wave-induced forces; and (v) nonlinear diffraction (e.g. Refs 1, 11–13, 16 and 33–41). The second-order forces can be expressed in terms of the second-order kernel, $h_f^{(2)}(\tau_1,\tau_2)$, or the quadratic transfer function $H_d^{(2)}(f_1,f_2)$. The hydrodynamic loads of potential origin can be conveniently expressed in the above format. The quadratization technique is necessary to express the second-order viscous load effects on TLPs. Since the potential effects do not require the quadratization procedure, the objective of this study could be met by just treating the drag-induced viscous loads. For this reason, the computationally efficient Morison equation was used for hydrodynamic loads instead of a combination of drag and potential effects from the Morison equation and diffraction theory.

The wave force is expressed in terms of the relative velocity by a modified form of the Morison equation for the drag force acting on the TLP in the surge direction,[1]

$$F_{\mathrm{wave}} = K_m\dot{u} + K_d\,|u+U-\dot{x}|\,(u+U-\dot{x}), \quad (4)$$

where $K_m = \rho C_m V_e$; $K_d = \frac{1}{2}\rho C_d A_e$. In this formulation, the first term represents inertial force and the second describes the viscous effects, where u, and $\dot{u}$ are water particle velocity and acceleration, respectively, and U is the current speed. Here, ρ is the water density, C_m and C_d are the inertia and drag coefficients which are usually determined from experimental data, and A_e and V_e are related to the area and volume of the submerged portion of the platform. The fluctuating water particle velocity, u, is characterized by a spectral representation wherein a Gaussian wave elevation spectrum, e.g. JONSWAP, Pierson–Moskowitz, etc. (e.g. Refs 1 and 2), is chosen to characterize a set of sea conditions and is related to the spectrum of u by a linear transfer function.

Unlike the wind force, the viscous wave force is not cast in a purely polynomial form, but must be so approximated for the implementation of the Volterra theory. Again, it is important to note that although the wave process may be assumed as Gaussian, the structural velocity in the preceding equations, due to its nature as a response to a nonlinear forcing function, is no longer Gaussian.

Equivalent statistical quadratization

In a quadratization approach, a statistically asymmetric nonlinear system having an arbitrary form is approximated by a second-order polynomial expression for analysis within the Volterra framework. In the approximate quadratic representation of the system the linear component is analogous to conventional statistical linearization while the retention of a second-order component gives the method its name.

The governing equation of a single-degree-of-freedom nonlinear system containing statistically asymmetric nonlinearities in both the system characteristics and the excitation may be written,

$$M\ddot{x} + C\dot{x} + Kx + g(x,\dot{x}) = f_L(v) + f_N(v,\dot{x}), \quad (5)$$

where M, C, and K are the structural mass, damping and stiffness, respectively, $g(x,\dot{x})$ represents a system nonlinearity, $f_L(v)$ and $f_N(v,\dot{x})$ represent the linear and nonlinear forcing terms, respectively, and v is the input wind velocity or water particle velocity process. The forthcoming discussion will outline the quadratization procedure.

Slow drift approximation

To eliminate the computational difficulty imposed by the non-Gaussian structural velocity, a slowly varying drift approximation is invoked. For a system with low natural frequency, the slowly varying drift motion plays an important role. This leads to a reasonable assumption, i.e. the higher-order nonlinear velocity terms can be neglected. As an example, the nonlinear terms in the wind and wave induced drag descriptions expanded in Taylor series in terms of the second-order component, $\dot{x}_2$, about the linear, Gaussian component, $\dot{x}_1$, are given by

$$(w + W - \dot{x})^2 \cong (w + W - \dot{x}_1)^2 - 2E[w + W - \dot{x}_1]\dot{x}_2, \tag{6}$$

$$\begin{aligned} |u + U - \dot{x}|(u + U - \dot{x}) &\cong |u + U - \dot{x}_1|(u + U - \dot{x}_1) \\ &- 2E[|u + U - \dot{x}_1|]\dot{x}_2. \end{aligned} \tag{7}$$

It is assumed as well that the second-order response itself is small compared to the first-order response and terms involving its higher-order powers may thus be neglected.

Splitting technique

Returning to eqn (5), we now expand the nonlinear functions in Taylor series in terms of the quadratic response and its velocity, and apply the assumptions of the previous section,

$$\begin{aligned} g(x, \dot{x}) &= g(x_1, \dot{x}_1) + \frac{\partial g(x_1, \dot{x}_1)}{\partial x}\frac{x_2}{2} + \frac{\partial g(x_1, \dot{x}_1)}{\partial \dot{x}}\frac{\dot{x}_2}{2} \\ &+ O(x_2^2, \dot{x}_2^2) \end{aligned}$$

$$g(x, \dot{x}) \approx g(x_1, \dot{x}_1) + \mu_{gx}\frac{x_2}{2} + \mu_{gv}\frac{\dot{x}_2}{2}, \tag{8}$$

where μ_{gx} and μ_{gv} are the expected values of the terms they replace. Similarly,

$$f_N(v, \dot{x}) = f_N(v, \dot{x}_1) + \frac{\partial f_N(v, \dot{x}_1)}{\partial \dot{x}}\frac{\dot{x}_2}{2} + O(\dot{x}_2^2),$$

$$f_N(v, \dot{x}) \approx f_N(v, \dot{x}_1) - \mu_{fv}\frac{\dot{x}_2}{2}. \tag{9}$$

By expanding in this way, two nonlinear functions of Gaussian processes (the initial terms on the right-hand sides of eqns (8) and (9)) remain along with two additional damping terms and an additional stiffness term.

Quadratization procedure

Since the two nonlinearities discussed in the previous section still have arbitrary forms, they must finally be approximated in terms of quadratic polynomials for the Volterra series technique to be effective. To this end, second-order approximations for both terms are written as,

$$\begin{aligned} g(x_1, \dot{x}_1) &\approx \tfrac{1}{2}(\beta_1 x_1^2 + \beta_2 x_1\dot{x}_1 + \beta_3\dot{x}_1^2) \\ f_N(v, \dot{x}_1) &\approx \sum_i \int_0^{L_i} dz\, \alpha_1(v - \dot{x}_1) \\ &+ \frac{1}{2}\sum_i \int_0^{L_i} dz\, \alpha_2(v - \dot{x}_1)^2, \end{aligned} \tag{10}$$

where the summation indicates the total excitation acting on each element of the structure. The unknown coefficients in eqns (10) are solved for by mean-square minimization of the following error terms,

$$\begin{aligned} \epsilon_g &= E[(g(x_1, \dot{x}_1) - \tfrac{1}{2}(\beta_1 x_1^2 + \beta_2 x_1\dot{x}_1 + \beta_3\dot{x}_1^2))^2], \\ \epsilon_f &= E\left[\left(f_N(v, \dot{x}_1) - \sum_i \int_0^{L_i} dz\, \alpha_1(v - \dot{x}_1)\right.\right. \\ &\left.\left. + \frac{1}{2}\sum_i \int_0^{L_i} dz\, \alpha_2(v - \dot{x}_1)^2\right)^2\right], \end{aligned} \tag{11}$$

which yields linear systems of algebraic equations. An advantage of the present technique is that none of the expected values computed in (11) involve non-Gaussian processes.

Now, letting,

$$a_1 = \sum_i \int_0^{L_i} dz\, \alpha_1 \quad \text{and} \quad a_2 = \sum_i \int_0^{L_i} dz\, \alpha_2,$$

an equivalent set of Volterra system equations can be written as,[26]

$$\begin{aligned} M\ddot{x}_1 + (C + a_1)\dot{x}_1 + Kx_1 &= f_L(v) + a_1 v, \\ M\ddot{x}_2 + (C + \mu_{gv} + \mu_{fv})\dot{x}_2 + (K + \mu_{gx})x_2 & \\ = a_2(v - \dot{x}_1)^2 - (\beta_1 x_1^2 + \beta_2 x_1\dot{x}_1 + \beta_3\dot{x}_1^2), \end{aligned} \tag{12}$$

for which the following transfer functions are derivable,

$$\begin{aligned} H_x^{(1)}(\omega) &= H_1(\omega)H_f^{(1)}(\omega), \\ H_{\dot{x}}^{(1)}(\omega) &= i\omega H_x^{(1)}(\omega), \\ H_v(\omega) &= H_\nu(\omega) - i\omega H_x^{(1)}(\omega), \\ &\text{(fluid–structure interaction term)} \\ H_x^{(2)}(\omega_1, \omega_2) &= H_2(\omega_1 + \omega_2)H_f^{(2)}(\omega_1, \omega_2), \\ H_{\dot{x}}^{(2)}(\omega_1, \omega_2) &= i(\omega_1 + \omega_2)H_x^{(2)}(\omega_1, \omega_2), \end{aligned} \tag{13}$$

where,

$$\begin{aligned} H_f^{(1)}(\omega) &= H_L(\omega) + a_1 H_\nu(\omega), \\ H_x^{(2)}(\omega_1, \omega_2) &= a_2 H_v(\omega_1)H_v(\omega_1) \\ &- \left(\beta_1 + \beta_2\frac{i(\omega_1 + \omega_2)}{2} + \beta_3\omega_1\omega_2\right) \\ &\times H_x^{(1)}(\omega_1)H_x^{(1)}(\omega_2) \end{aligned}$$

and

$$H_1(\omega) = [K - \omega^2 M + i\omega(C + a_1)]^{-1},$$

$$H_2(\omega) = [(K + \mu_{gx}) - \omega^2 M + i\omega(C + \mu_{gv} + \mu_{fv})]^{-1}.$$

In future developments, the following relationships will be helpful,

$$H_x^{(1)*}(\omega) = H_x^{(1)}(-\omega),$$

$$H_x^{(2)*}(\omega_1, \omega_2) = H_x^{(2)}(-\omega_1, -\omega_2). \tag{14}$$

Response statistics

In the present case the response distribution is no longer Gaussian, therefore, higher-order moments or cumulants are needed to describe the response statistics. The response statistics are considered in terms of the response cumulants, k_i, rather than the moments. The first-order cumulant is the mean of the response and the second-order cumulant is equal to its variance. The third- and fourth-order cumulants are descriptors of the skewness and kurtosis, respectively, of the process, quantifying its departure from Gaussianity. The skewness and kurtosis are given by

$$\gamma_3 = \frac{k_3}{k_2^{3/2}}; \qquad \text{and} \qquad \gamma_4 = \frac{k_4}{k_2^2}. \tag{15}$$

The power spectrum and the first four cumulants can be obtained from the following,[21]

$$D_x(\omega) = k_1\delta(\omega) + |H_x^{(1)}(\omega)|^2 D(\omega) + \frac{1}{2}\int_{-\infty}^{\infty} |H_x^{(2)}(\theta, \omega-\theta)|^2 D(\theta) D(\omega-\theta)\, d\theta. \tag{16}$$

where the transfer functions are as defined in the previous section, $D_x(\omega)$ is the two-sided spectrum of $x(t)$; and $D(\omega)$ represents the two-sided spectrum of $v(t)$.

For brevity's sake, let $H_x^{(1)}(1)$, $H_x^{(2)}(1,2)$, $D(1)$ represent $H_x^{(1)}(\omega_1)$, $H_x^{(2)}(\omega_1,\omega_2)$ and $D(\omega_1)\,d\omega_1$, respectively. The associated cumulants are given below

$$k_1 = x_0 + \frac{1}{2}\int_{-\infty}^{\infty} H_x^{(2)}(1,-1)D(1),$$

$$k_2 = \int_{-\infty}^{\infty} H_x^{(1)}(1) H_x^{(1)}(-1) D(1) + \frac{1}{2}\int_{-\infty}^{\infty}\int_{-\infty}^{\infty} H_x^{(2)}(1,2) H_x^{(2)}(-1,-2) D(1) D(2),$$

$$k_3 = 3\int_{-\infty}^{\infty}\int_{-\infty}^{\infty} H_x^{(1)}(1) H_x^{(1)}(2) H_x^{(2)}(-1,-2) D(1) \times D(2) + \int_{-\infty}^{\infty}\int_{-\infty}^{\infty}\int_{-\infty}^{\infty} H_x^{(2)}(1,2) H_x^{(2)}(-1,3) \times H_x^{(2)}(-2,-3) D(1) D(2) D(3),$$

$$k_4 = 12\int_{-\infty}^{\infty}\int_{-\infty}^{\infty}\int_{-\infty}^{\infty} H_x^{(1)}(1) H_x^{(1)}(2) H_x^{(2)}(-1,3) \times H_x^{(2)}(-2,-3) D(1) D(2) D(3) + 3\int_{-\infty}^{\infty}\int_{-\infty}^{\infty}\int_{-\infty}^{\infty}\int_{-\infty}^{\infty} H_x^{(2)}(1,2) H_x^{(2)}(-1,3) \times H_x^{(2)}(-2,4) H_x^{(2)}(-3,-4) D(1) D(2) D(3) D(4), \tag{17}$$

where x_0 in the expression for k_1 is the static response.

In general, expressions for the response cumulants of Volterra systems are not available. Inspecting eqns (17), even for the present case in which only terms up to the second order are treated, the higher order cumulant expressions become increasingly complex. In the sections to follow, two methods for evaluating higher-order cumulants will be discussed.

Direct integration method

The calculation of the fourth-order cumulant was considered prohibitive, not only because of the behavior of the integrand, but also due to very extensive computational effort needed in evaluating the multi-fold integrals. Bedrosian and Rice[21] stated that the four-fold integral in the above equations cannot be carried out because of its complexity. Recently, Spanos and Donley (e.g. Ref. 13) reported a similar difficulty. The present paper simplifies the evaluation of the four-fold integral by reducing it into a three-fold integral.

To further assist in factorizing the more complicated integrals, the following one- and two-dimensional transfer functions may be developed,

$$C_{10}(\omega) = H_x^{(1)}(\omega),$$

$$C_{11}(\omega) = \int_{-\infty}^{\infty} H_x^{(1)}(\alpha) H_x^{(2)}(-\alpha,\omega) D(\alpha)\, d\alpha,$$

$$C_{20}(\omega_1,\omega_2) = H_x^{(2)}(\omega_1,\omega_2),$$

$$C_{22}(\omega_1,\omega_2) = \int_{-\infty}^{\infty} H_x^{(2)}(\alpha,\omega_1) H_x^{(2)}(-\alpha,\omega_2) D(\alpha)\, d\alpha, \tag{18}$$

noting that $C_{11}(-\omega) \neq C_{11}^*(\omega)$ and $C_{22}(\omega_1,\omega_2)$ is Hermitian, i.e. $C_{22}(\omega_1,\omega_2) = C_{22}^*(\omega_2,\omega_1)$. Then, the cumulant expressions of (17) can be recast in the following manner,

$$k_1 = x_0 + \frac{1}{2}\int_{-\infty}^{\infty} C_{20}(1,-1) D(1),$$

$$k_2 = \int_{-\infty}^{\infty} |C_{10}(1)|^2 D(1) + \frac{1}{2}\int_{-\infty}^{\infty}\int_{-\infty}^{\infty} |C_{20}(1,2)|^2 D(1) D(2),$$

$$k_3 = 3\int_{-\infty}^{\infty} C_{10}(1)\,C_{11}(-1)\,D(1) + \int_{-\infty}^{\infty}\int_{-\infty}^{\infty} C_{20}(-1,-2)\,C_{22}(1,2)\,D(1)\,D(2),$$
$$k_4 = 12\int_{-\infty}^{\infty} |C_{11}(1)|^2 D(1) + 3\int_{-\infty}^{\infty}\int_{-\infty}^{\infty} |C_{22}(1,2)|^2 D(1)\,D(2). \quad (19)$$

By this approach, the solution of the fourth-order cumulant involves an effort equal to that needed for solving the third-order cumulant without any compromise on the accuracy.

Kac–Siegert technique

A second approach to evaluating response cumulants is named after Kac and Siegert who first applied it to the theory of noise in radio receivers with square law detectors in 1947.[22] In fact, it may be taken as the generalized Fourier series representation method,[42] based on the theory of linear integral equations. Its application to ocean engineering problems has been reported in Refs 43–46. The following is a formulation of the response cumulants up to fourth-order obtained by employing the Kac–Siegert technique in the context of quadratization.

The generalized Fourier series expansion can be written in one- and two-dimensional forms,

$$Q_1(x) \cong \sum_{i=1}^{\infty} \alpha_i \phi_i(x),$$
$$Q_2(x,y) \cong \sum_{i=1}^{\infty}\sum_{j=1}^{\infty} \beta_{ij}\phi_i(x)\,\phi_j^*(y). \quad (20)$$

The above expression is sometimes called the degenerate kernel or separable kernel within the theory of integral equations. In the case when the second-order transfer function, $Q_2(x,y)$, is Hermitian, the basis functions, $\phi_i(.)$, are chosen as the characteristic functions of the following Fredholm homogeneous integral equation of second kind,

$$\int_a^b Q_2(x,y)\,\phi(y)\,dy = \lambda\phi(x). \quad (21)$$

The nontrivial eigenvalues of eqn (21) are real and corresponding eigenfunctions are orthogonal to one another, i.e. $(\phi_i,\phi_j) = \delta_{ij}$. Due to this orthogonality, $Q_2(x,y)$ may be recast as,

$$Q_2(x,y) = \sum_{i=1}^{\infty} \lambda_i\phi_i(x)\,\phi_i^*(y), \quad (22)$$

the convergence of which can be shown by Hilbert's and Mercer's theorems.[42]

For the present application, the second-order system function is

$$Q_2(x,y) = G(x)\,H_x^{(2)}(x,-y)\,G(y), \quad (23)$$

where $G(x) = D(x)^{1/2}$, and $Q_2(x,y)$ is Hermitian. Both x and y represent frequencies, which are discretized as $\{\omega_i, i = 1,2,\ldots,N\}$, with equal intervals Δ.

The discrete form of the homogeneous integral equation constitutes a linear algebraic eigenvalue problem as follows,

$$\sum_{j=1}^{N} Q_2(\omega_i,\omega_j)\,W_j\phi(\omega_j)\,\Delta + \sum_{j=1}^{N} Q_2(\omega_i,-\omega_j)\,W_j\phi(-\omega_j)\,\Delta = \lambda\phi(\omega_i), \quad (24)$$

$$\sum_{j=1}^{N} Q_2(-\omega_i,\omega_j)\,W_j\phi(\omega_j)\,\Delta + \sum_{j=1}^{N} Q_2(-\omega_i,-\omega_j)\,W_j\phi(-\omega_j)\,\Delta = \lambda\phi(-\omega_i), \quad (25)$$

where W_j are the weighting factors determined by the numerical method used to evaluate these equations. For slowly varying drift response applications, Naess[45] employed Newman's approximation[33] and ignored the interaction terms at sum frequencies, thus the second term in eqn (24) and the first term in eqn (25) may be eliminated. However, this assumption, though valid for slow drift response, is not applicable in the case of response due to wind loads. The preceding equations can be solved numerically to obtain the eigenvalues and the corresponding eigenvectors (see Appendix A). Then, the system transfer functions can be obtained as,

$$G(\omega_1)\,H_x^{(2)}(\omega_1,-\omega_2)\,G(\omega_2) = \sum_{i=1}^{N} \lambda_i\phi_i(\omega_1)\,\phi_i^*(\omega_2),$$
$$H_x^{(1)}(\omega)\,G(\omega) = \sum_{j=1}^{N} \alpha_j\phi_j(\omega), \quad (26)$$

where, $\alpha_j = \int_{-\infty}^{\infty} H_x^{(1)}(\omega)\,G(\omega)\,\phi_j^*(\omega)\,d\omega$.

Substituting these expressions into eqns (17) leads to the following description of the cumulants:

$$k_1 = x_0 + \frac{1}{2}\sum_{i=1}^{M}\lambda_i,$$
$$k_2 = \sum_{i=1}^{M}\alpha_i^2 + \frac{1}{2}\sum_{i=1}^{M}\lambda_i^2,$$
$$k_3 = 3\sum_{i=1}^{M}\alpha_i^2\lambda_i + \sum_{i=1}^{M}\lambda_i^3, \text{ and}$$
$$k_4 = 12\sum_{i=1}^{M}\alpha_i^2\lambda_i^2 + 3\sum_{i=1}^{M}\lambda_i^4, \quad (27)$$

where the series expressions are truncated after M terms.

It has been observed that the number of terms, M, required for convergence is related to the system damping.[19] Indeed, for larger damping fewer terms need to be retained.

A notable advantage of the Kac–Siegert approach is that it provides information on the cumulants higher than the fourth order. Usually, however, only the third- and fourth-order cumulants are significant and possess physical interpretations in terms of skewness and kurtosis.

Time-domain simulation

The procedures laid out herein have been verified via a Monte Carlo simulation technique given a prescribed power spectrum, $S(\omega)$, for a random process, $\zeta(t)$. Sample time histories of either the wind or the wave process, given the appropriate spectral representation, may be generated according to,

$$\zeta(t) = \sum_{j=1}^{N} \sqrt{(2S(\omega_j)\,\Delta\omega_j)}\cos(\omega_j t + \theta_j), \tag{28}$$

where θ_j are independent random phases distributed uniformly between 0 and 2π, and $\omega_j = j\,\Delta\omega$. Consideration should be given to appropriately choosing $\Delta\omega$ to suitably discretize the particular spectrum of the process being simulated, paying close attention to the trade-off in terms of time resolution and the overall system dynamics. The efficiency of this simulation procedure may be boosted significantly by employing a fast Fourier transform method (e.g. Refs 48 and 49).

Combined wind, wave and current effects

Typically, wind and wave loadings impinge concurrently on a TLP in a given ocean environment. Indeed, wind plays a part in generating waves but the exact correlation between wind velocity fluctuations and wave elevations has not yet been formalized. Herein, the combined effect of wind and waves is viewed through structural response motions. If we assume: (i) that the total response is simply the sum of the response due to wave loading and the response due to wind loading; (ii) the wind loading is small relative to the wave loading; (iii) the response velocity due to wind loading is small relative to the response velocity due to wave loading, the equations of motion due to combined wind, wave and current loadings are given by

$$\begin{aligned} &M\ddot{x}^{\text{wind}} + (C + C_{\text{wave}})\dot{x}^{\text{wind}} + Kx^{\text{wind}} \\ &\quad = K_{\text{w}}(w + W - \dot{x}^{\text{wind}})^2, \\ &M\ddot{x}^{\text{wave}} + (C + C_{\text{wind}})\dot{x}^{\text{wave}} + Kx^{\text{wave}} \\ &\quad = K_{\text{m}}\dot{u} + K_{\text{d}}\,|u + U - \dot{x}^{\text{wave}}|(u + U - \dot{x}^{\text{wave}}), \end{aligned} \tag{29}$$

where $C_{\text{wind}} = -E[\partial f_{\text{wind}}/\partial\dot{x}]$ and $C_{\text{wave}} = -E[\partial f_{\text{wave}}/\partial\dot{x}]$ denote the damping introduced by the wind loads and wave loads, f_{wind} and f_{wave}, respectively.

The solution of the preceding equations is obtained following the two procedures outlined earlier in the text. Based on the assumptions made earlier, the total response cumulants can be obtained by a simple summation of the response cumulants due to all loadings, (e.g. Ref. 47)

$$k_{\text{m}}^{\text{total}} = k_{\text{m}}^{\text{wind}} + k_{\text{m}}^{\text{wave}}, \qquad m = 1, 2, 3, 4, \ldots \tag{30}$$

Probability distribution of response

Following the evaluation of the first four moments or cumulants of response, the non-Gaussian distribution of response processes can be obtained with a subsequent estimation of the extreme value distribution. In this study, Gram–Charlier Series, Hermite Moment Approach and Maximum Entropy method are utilized. A short description of each is given in Appendix B.

EXAMPLE

To illustrate the nonlinear effects introduced by wind and wave loads, an idealized TLP model is utilized. Since the wind force is already in a quadratic form, it is readily cast as an equivalent Volterra system[19] and only the wave drag force is treated rigorously here. First, the splitting technique is performed whereby the nonlinearity in the right side of eqn (4) is expanded as follows in a Taylor series in terms of second order response velocity,

$$\begin{aligned} |u + U + \dot{x}|(u + U + \dot{x}) &= |u + U + \dot{x}_1|(u + U + \dot{x}_1) \\ &\quad - 2\,|u + U + \dot{x}_1|\frac{\dot{x}_2}{2} + O(\dot{x}_2^2). \end{aligned} \tag{31}$$

The slow drift approximation is employed, and in order to eliminate a time-dependence of the additional damping term on the right-hand side of eqn (31), the coefficient is approximated by its expected value, i.e.

$$\begin{aligned} |u + U + \dot{x}|(u + U + \dot{x}) &\approx |u + U + \dot{x}_1|(u + U + \dot{x}_1) \\ &\quad - 2E[\,|u + U + \dot{x}_1|\,]\frac{\dot{x}_2}{2}. \end{aligned} \tag{32}$$

Since the initial term on the right-hand side in eqn (32) is not cast in a polynomial form and as such is not yet tractable by the Volterra approach, the quadratization procedure is now invoked to approximate it in terms of the relative fluid–structure velocity as follows,

$$\begin{aligned} |u + U + \dot{x}_1|(u + U + \dot{x}_1) &\approx \alpha_0 + \alpha_1(u - \dot{x}_1) \\ &\quad + \alpha_2(u - \dot{x}_1)^2. \end{aligned} \tag{33}$$

The polynomial approximation of eqn (33) may then be tailored by minimizing the mean-square of the following

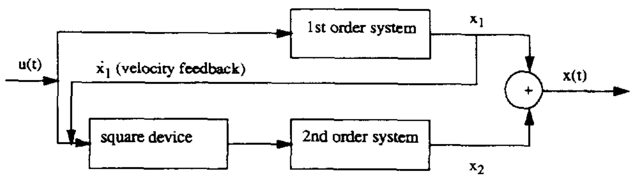

Fig. 1. Schematic of equivalent Volterra system for a TLP under nonlinear loading.

error term,

$$\epsilon = |u + U - \dot{x}_1|(u + U - \dot{x}_1) - \alpha_0 - \alpha_1(u - \dot{x}_1) - \alpha_2(u - \dot{x}_1)^2. \quad (34)$$

This minimization produces a system of three equations for the unknowns, α_i,

$$\begin{bmatrix} 1 & 0 & \sigma^2 \\ 0 & \sigma^2 & 0 \\ \sigma^2 & 0 & 3\sigma^4 \end{bmatrix} \begin{bmatrix} \alpha_0 \\ \alpha_1 \\ \alpha_2 \end{bmatrix} = \begin{bmatrix} E[|u + U - \dot{x}_1|(u + U - \dot{x}_1)] \\ E[(u - \dot{x}_1)|u + U - \dot{x}_1|(u + U - \dot{x}_1)] \\ E[(u - \dot{x}_1)^2|u + U - \dot{x}_1|(u + U - \dot{x}_1)] \end{bmatrix}, \quad (35)$$

which when solved yields,

$$\alpha_0 = 2U\sigma(rb_1 + b_2); \quad \alpha_1 = 4\sigma(rb_1 + b_2), \quad \text{and} \quad \alpha_2 = 2b_1, \quad (36)$$

where

$$b_1 = \frac{1}{\sqrt{2\pi}} \int_0^r \exp\left(-\frac{y^2}{2}\right) dy,$$

$$b_2 = \frac{1}{\sqrt{2\pi}} \exp\left(-\frac{r^2}{2}\right); \quad r = \frac{U}{\sigma}; \quad \text{and}$$

$$\sigma^2 = E[(u - \dot{x}_1)^2].$$

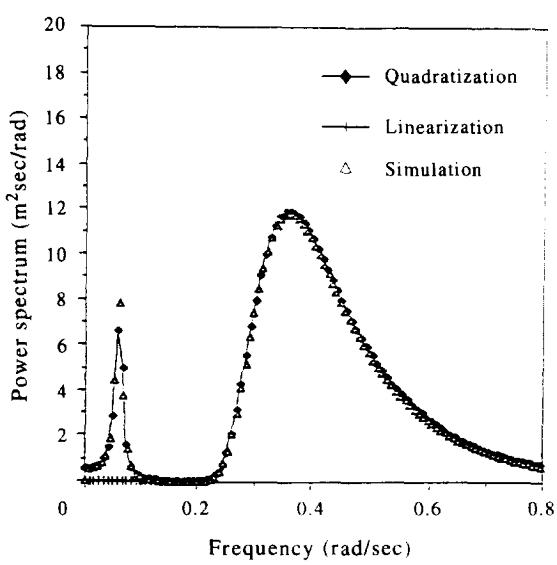

Fig. 2. TLP response spectrum due to wave loading ($U = 0{\cdot}4$ m/s).

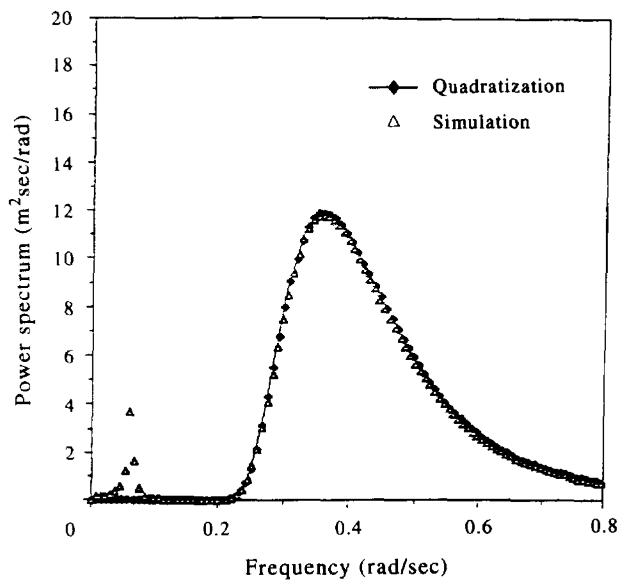

Fig. 3. TLP response spectrum due to wave loading ($U = 0{\cdot}0$ m/s).

Turning attention back the system (35), an important advantage of the present technique may be noted in the fact that all of the expected values taken involve only Gaussian quantities and functions thereof. A more detailed treatment of the expected values in the right-hand-side vector is given in Appendix C.

Now the equations of motion for wave excitation can be expressed as

$$M\ddot{x}_1 + (C + a_1)\dot{x}_1 + Kx_1 = K_m\dot{u} + a_1 u,$$

$$M\ddot{x}_1 + (C + a_1)\dot{x}_2 + Kx_2 = \frac{a_2}{2}(u - \dot{x}_1)^2, \quad (37)$$

where $a_0 = K_d\alpha_0$; $a_1 = K_d\alpha_1$; and $a_2 = 2K_d\alpha_2$. A schematic of this system is given in Fig. 1. The static

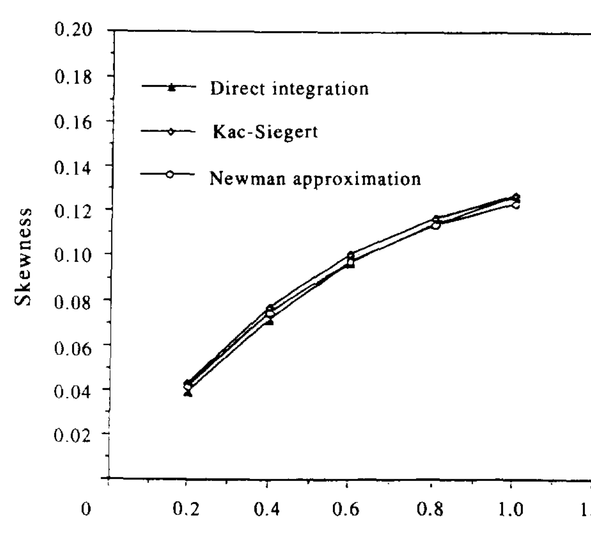

Fig. 4. Skewness of TLP response due to wave loading as it varies with current speed.

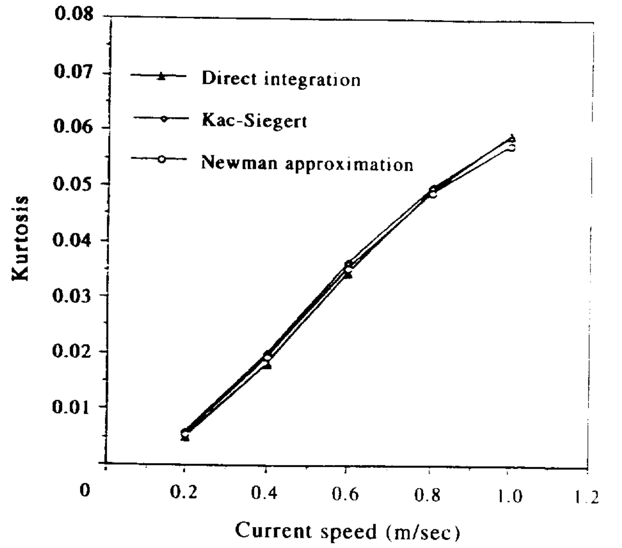

Fig. 5. Kurtosis of TLP response due to wave loading as it varies with current speed.

response of this system may be given as,

$$x_0 = \frac{a_0}{K} \qquad (38)$$

It is then desired to characterize the time-varying system response in the frequency domain. Thus, the following transfer functions are developed to relate x_1, $(u - \dot{x}_1)$, and x_2, respectively, to the input water particle velocity spectrum

$$H_x^{(1)}(\omega) = (K_m i\omega + a_1)H(\omega),$$
$$H_v(\omega) = 1 - i\omega H_x^{(1)}(\omega). \qquad (39)$$

$$H_x^{(2)}(\omega_1, \omega_2) = a_2 H(\omega_1 + \omega_2) H_v(\omega_1) H_v(\omega_2), \qquad (40)$$

where $H(\omega) = [K - \omega^2 M + i\omega(C + a_1)]^{-1}$. The cumulants of the response based on these frequency domain formulations are given in the earlier discussion.

Similarly, the equations of motion under the wind force are given by

$$M\ddot{x}_1 + (C + a_1)\dot{x}_1 + Kx_1 = a_1 w,$$
$$M\ddot{x}_2 + (C + a_1)\dot{x}_2 + Kx_2 = \frac{a_2}{2}(w - \dot{x}_1)^2, \qquad (41)$$

where $a_0 = K_w W^2$; $a_1 = 2K_w W$; and $a_2 = 2K_w$. The static response has the same form as eqn (38) and the transfer function for x_1, now has the form,

$$H_x^{(1)}(\omega) = a_1 H(\omega). \qquad (42)$$

The transfer functions for $(w - \dot{x}_1)$ and x_2 maintain the same form as H_v and $H_x^{(2)}$ in eqn (40). Finally, note in eqns (37) and (41) the presence of terms containing $(u - \dot{x}_1)^2$ and $(w - \dot{x}_1)^2$ which are squares of Gaussian fluid–structure interaction processes and include nonlinear damping terms.

The TLP is modeled as a single degree of freedom system with structural and added mass, $M = 7{\cdot}1286 \times 10^7$ kg, stiffness, $K = 2{\cdot}8143 \times 10^5$ N/m and a structural damping ratio, $C/2M\omega_N$, of 0·05. Also, $K_m = 4 \times 10^7$ and $K_d = 6 \times 10^5$ are the inertia and drag coefficients, respectively. The input wave elevation spectrum is modelled by a Pierson–Moskowitz spectrum characterized by a significant wave height of 12 m and a peak frequency of 0·395 rad/s, well above the resonance region for the TLP surge mode. Nonetheless, Figs 2

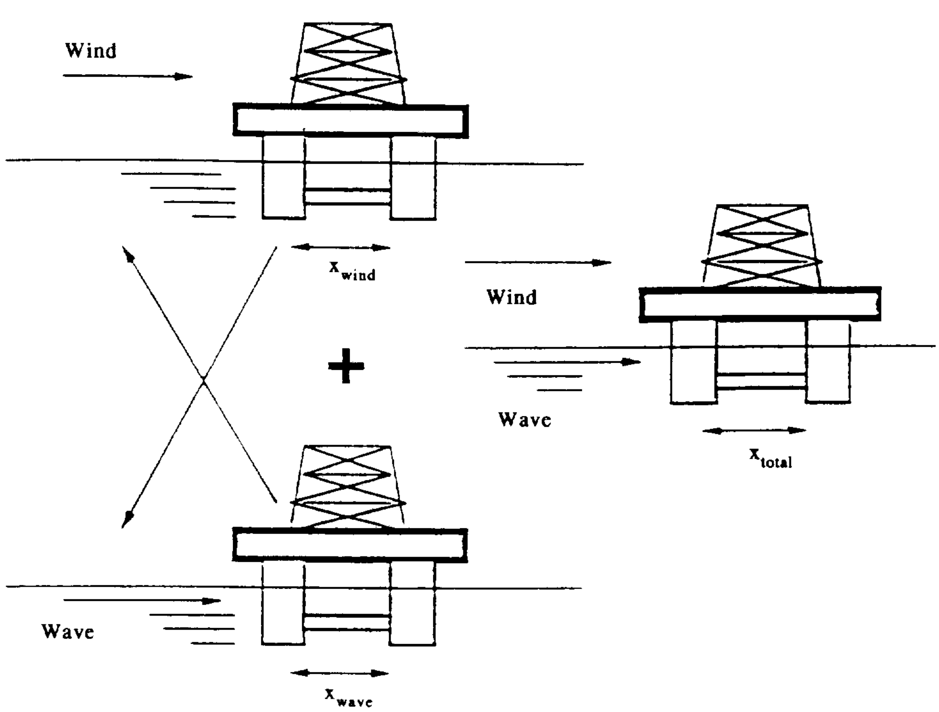

Fig. 6. Schematic of wind wave interaction on a TLP.

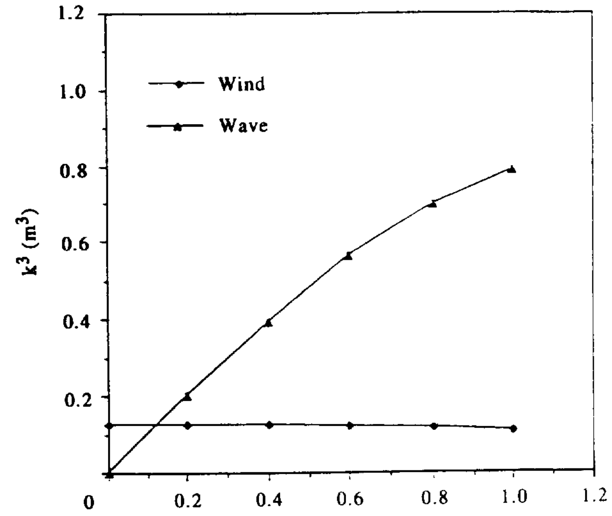

Fig. 7. Third-order cumulant of TLP response due separately to wind and wave loadings.

and 3 indicate a surge response peak due to the second order forces in the resonance region of the TLP which is captured by the quadratization technique in the first figure, but is not seen in the response obtained from linearization. The same figures also illustrate that the presence of currents increases the quadratic contribution. Figure 3, which illustrates the case when no current is present, reveals the limitation of the quadratization technique. That is, the procedure degenerates to linearization when the nonlinearity becomes statistically symmetric. Nevertheless, this type of higher-order response energy may be captured by a cubicization approach[17,20] which is beyond the scope of this study.

Application of three techniques, direct integration, Kac–Siegert approach, and Newman's approximation,[45] to obtain the skewness and kurtosis of the response to

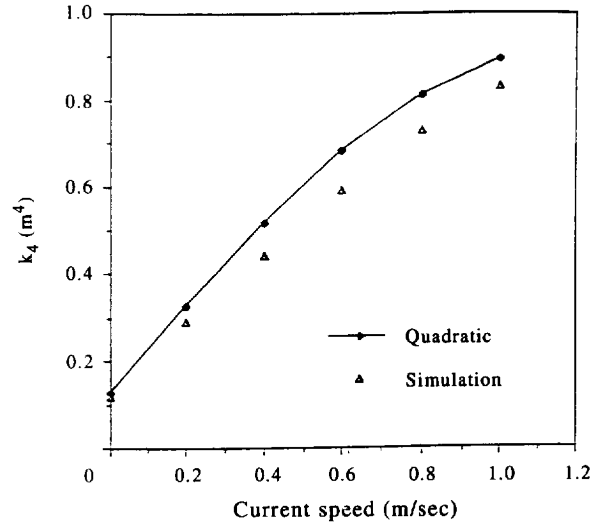

Fig. 9. Third-order cumulant of TLP response due to combined wind–wave loading.

eqn (37) is illustrated in Figs 4 and 5. The graphical similarity of all results in these figures indicates that Newman's approximation, which ignores sum frequency contributions of the second-order force, is adequate for analyzing TLP surge response due to wave loads.

Figure 6 is a schematic of a TLP under the influence of concurrent wind and wave loadings, i.e. a combination of eqns (37) and (41) as described in the earlier discussion. For this example, we assume a mean wind speed of 20 m/s and $K_w = 1250$. In Figs 7 and 8, the third- and fourth-order response cumulants are given over a range of current speeds. Clearly, from these illustrations, the wave load effects are dominant over those due to wind loads in terms of higher-order TLP response statistics. The combined response cumulants due to both wind and wave loads compare acceptably to those obtained via numerical simulation in Figs 9 and

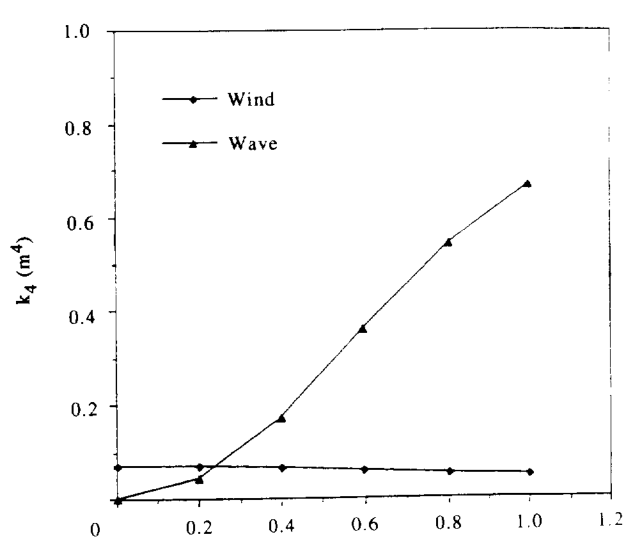

Fig. 8. Fourth-order cumulant of TLP response due separately to wind and wave loadings.

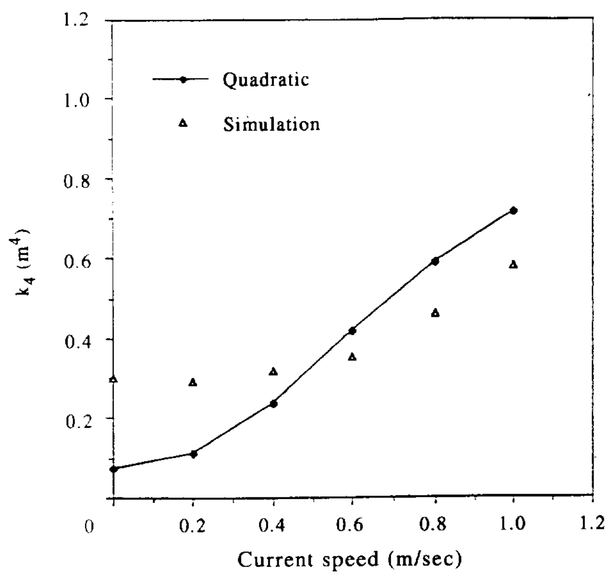

Fig. 10. Fourth-order cumulant of TLP response due to combined wind–wave loading.

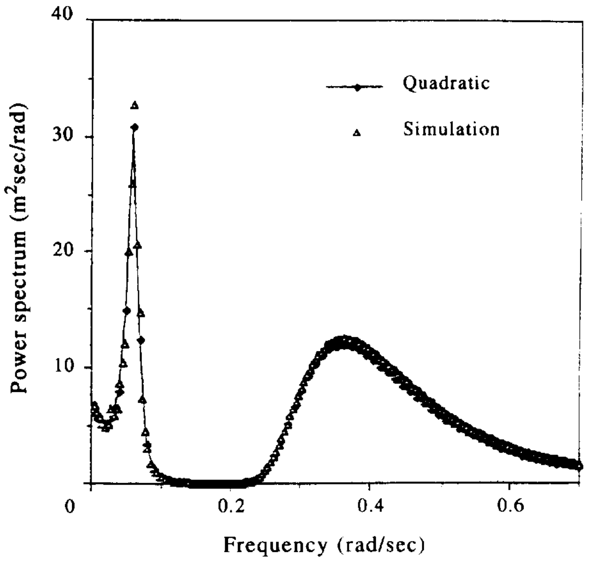

Fig. 11. TLP response due to combined wind–wave loading ($U = 0{\cdot}4$ m/s).

10, thus supporting the use of the simplified, wind–wave combination model proposed in this study. Comparing the spectrum of Fig. 11 to that of Fig. 2, it is observed that the dynamics of the wind produce a significant low frequency peak in the response of the combined system. The low frequency peak diminishes with increasing current speed, indicating the importance of the hydrodynamic damping introduced by larger currents on the wind load response of the system. More detail is given in Ref. 32.

The response statistics obtained through application of the quadratization technique are useful in characterizing the overall distribution and crossing rates of the non-Gaussian response. Figure 12 is the probability distribution of the response due to the combination of wind and wave loading. In this figure, the departure from Gaussianity is readily evident in the tails of

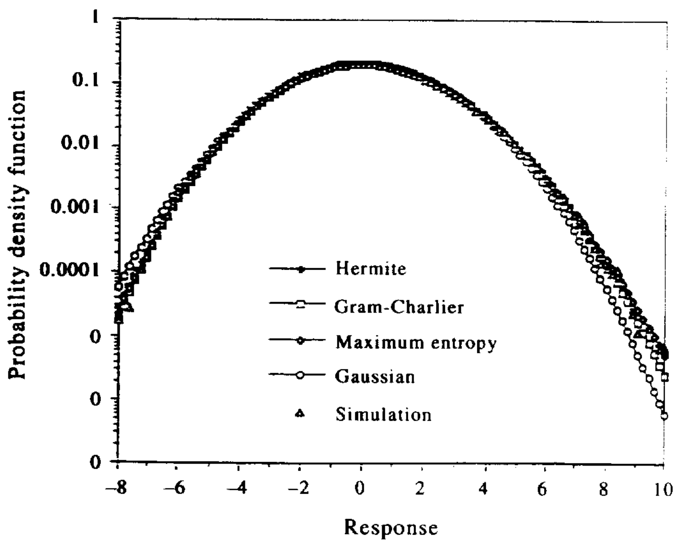

Fig. 12. PDF of TLP response due to combined wind–wave loading.

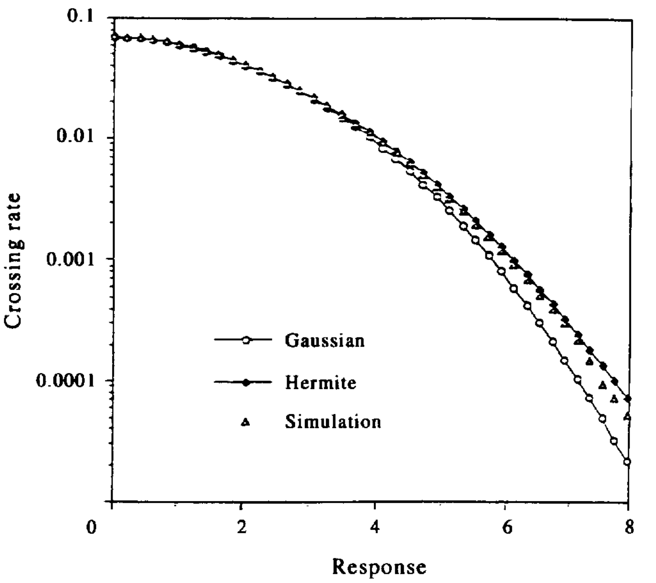

Fig. 13. Crossing rates of the TLP response process due to wind–wave loading.

the distribution and is captured by including the higher-order cumulant information gleaned from the present techniques in the probability density approximations. The best approximations seem to be given in these figures by the moment-based Hermite method and the maximum entropy method. The ability to characterize the tail contributions of these probability density functions will greatly enhance the accuracy of the prediction of response extremes. Indeed, Fig. 13 illustrates favorable approximation of the crossing rate of the system response to combined wind and wave loading by the moment-based Hermite approximation. Further, Fig. 14 exemplifies the difference between the peak distribution of the non-Gaussian response to wave loads and a similar Gaussian response.

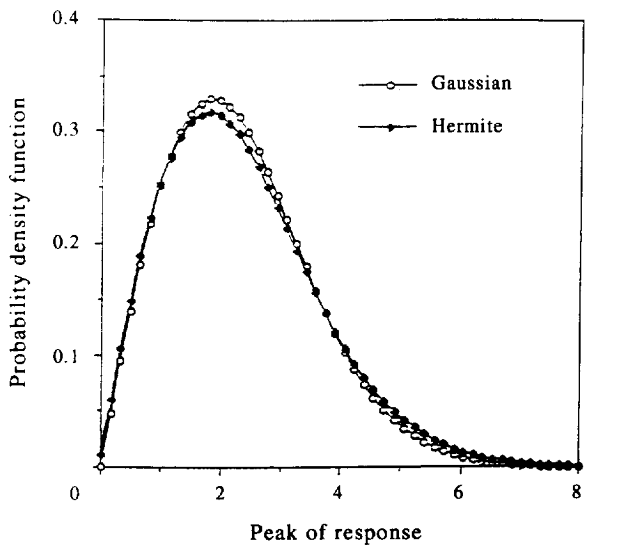

Fig. 14. Distribution of TLP response maxima due to wave load.

CONCLUDING REMARKS

The quadratization approach presented in this paper addresses the treatment of nonlinearities in the frequency domain analysis that result from wind and wave loadings on TLPs. The results obtained in terms of TLP response spectra and cumulants are in good agreement with simulation results. The higher-order cumulants are used to determine the response probability distributions and crossing rates using available approximating techniques. The subsequently derived response distributions are also in good agreement with simulated results. For the case when the nonlinearity in question is statistically symmetric, e.g. waves with no current, the quadratization technique reduces, in effect, to linearization. To address this, a cubicization technique which involves recasting the response in this case as the sum of the outputs of a first-order and a third-order Volterra system will be presented in a future work.

ACKNOWLEDGEMENTS

The support for this study was provided in part by NSF grant BCS-9096274 and ONR Grant No. 00014-93-1-0761.

REFERENCES

1. Chakrabarti, S. K., *Hydrodynamics of Offshore Structures*. Springer-Verlag, New York, 1987.
2. Sarpkaya, T. & Issacson, M., *Mechanics of Wave Forces on Offshore Structures*. Van Nostrand Reinhold, 1981.
3. Lin, Y. K., *Probabilistic Theory of Structural Dynamics*, Robert E. Krieger Publishing Company, Huntington, NY. 1976.
4. Roberts, J. B. & Spanos, P. D., *Random Vibration and Statistical Linearization*. John Wiley, New York, 1990.
5. Soong, T. T. & Grigoriu, M., *Random Vibration of Mechanical and Structural Systems*. Prentice-Hall, Inc., Englewood Cliffs, NJ, 1993.
6. Borgman, L. E., Spectral analysis of ocean wave forces on pilings. *Journal of Waterways and Harbors Division, ASCE*, **93**(WW2) (1967) 129–156.
7. Eatock-Taylor, R. & Rajagopalan, A., Load spectra for slender offshore structures in waves and currents. *Earthquake Engineering and Structural Dynamics*, **11** (1983) 831–842.
8. Tuah, H. & Hudspeth, R. R., Non-deterministic wave force on fixed small vertical piles. *Applied Ocean Research*, **5** (1983) 63–68.
9. Grigoriu, M., Extremes of wave forces. *Journal of Engineering Mechanics, ASCE*, **110**(12) (1984) 1731–1742.
10. Yuan, Y. & Tung, C. C., Application of Hermite polynomials to wave and wave force statistics. *Ocean Engineering*, **11**(6) (1984) 593–607.
11. Kareem, A. & Li, Y., Stochastic response of tension leg platforms to wind and wave fields. Technical Report No. UHCE88-18, Department of Civil Engineering, University of Houston, TX, 1988.
12. Li, Y. & Kareem, A., Stochastic response of a tension leg platform to wind and wave fields. *Journal of Wind Engineering and Industrial Aerodynamics*, **36** (Dec.) (1990) 915–920.
13. Donley, M. G. & Spanos, P. D., *Dynamic Analysis of Nonlinear Structures by the Method of Statistical Quadratization, Lecture Notes in Engineering*. Springer-Verlag, New York, 1990.
14. Spanos, P. D. & Donley, M. G., Stochastic response of a tension leg platform to viscous drift forces. *Proceedings of the 9th OMAE Conference, ASME*, Houston, TX, 1990.
15. Spanos, P. D. & Donley, M. G., Equivalent statistical quadratization for nonlinear systems. *Journal of Engineering Mechanics, ASCE*, **117**(6) (1991) 1289–1309.
16. Kareem, A. & Hsieh, C. C., Probabilistic response analysis of offshore platforms to wave loads. Technical Report CEND 91-1, Department of Civil Engineering, University of Notre Dame, IN, 1991.
17. Kareem, A. & Zhao, J., Stochastic response analysis of tension leg platforms: A statistical quadratization and cubicization approach. *Proceedings of the OMAE '94 Conference, Vol. I, ASME*, New York, 1994.
18. Kareem, A. & Zhao, J., Response statistics of tension leg platforms to wind and wave loadings. Technical Report No. NDCE93-002, Department of CE/GEOS, University of Notre Dame, IN, 1993.
19. Kareem, A. & Zhao, J., Analysis of non-gaussian surge response of tension leg platforms under wind loads. *Journal of Offshore Mechanics and Arctic Engineering*, **116** (1994) 137–144.
20. Tognarelli, M. A., Kareem, A., Zhao, J. & Rao, K. B., Quadratization and cubicization: Analysis tools for offshore engineering. *Proceedings of the Tenth ASCE Engineering Mechanics Specialty Conference*, Boulder, CO, 1995.
21. Bedrosian, E. and Rice, S., The output properties of volterra systems (Nonlinear systems with memory) driven by harmonic and Gaussian inputs. *Proceedings of IEEE*, **59**(12) (1971) 1688–1707.
22. Kac, M. & Siegert, A., On the theory of noise in radio receivers with square law detectors. *Journal of Applied Physics*, **18** (1947) 1688–1707.
23. Winterstein, S., Non-normal responses and fatigue damage. *Journal of Engineering Mechanics*, **111**(10) (1985) 1291–1295.
24. Wiener, N., Response of a nonlinear device to noise. Report No. 129, Radiation Laboratory, MIT, Cambridge, MA, 1942.
25. Barrett, J. F., The use of functionals in the analysis of nonlinear physical systems. *Journal of Electronics and Control*, **15**(6) (1963) 567–615.
26. Schetzen, M., *The Volterra and Wiener Theories of Nonlinear Systems*. John Wiley, New York, 1980.
27. Kareem, A. & Dalton, C., Dynamic effects of wind on tension leg platforms. *Proceedings of the Ocean Structural Dynamics Symposium '82*, Oregon State University, Corvallis, OR, 1982.
28. Simiu, E. & Leigh, S.D., Turbulent wind and tension leg platform surge. *Journal of Structural Engineering, ASCE*, **110**(4) (1984) 785–802.
29. Kareem, A., Nonlinear dynamic analysis of compliant offshore platforms subjected to fluctuating wind. *Journal of Wind Engineering and Industrial Aerodynamics*, **14** (1983) 345–356.
30. Vickery, P. J., Wind and wave loads on a tension leg platform: Theory and experiment. *Journal of Wind Engineering and Industrial Aerodynamics*, **36** (1990) 905–914.

31. Kareem, A., Wind induced response analysis of tension leg platforms. *Journal of Structural Engineering*, **111**(1) (1985) 37–55.
32. Kareem, A., Zhao, J. & Tognarelli, M. A., Surge response statistics of tension leg platforms under wind and wave loads: A statistical quadratization approach. Technical Report No. NDCE95-001, Department of CE/GEOS, University of Notre Dame, IN, 1995.
33. Newman, J.N., Second order slowly varying forces in irregular waves. *Proc. Int. Symp. on Dynamics of Marine Vehicles and Offshore Structures in Waves.* University College London, London, (1974) 182–186.
34. Pinkster, J. A., Mean and low frequency wave drifting forces on floating structures. *Ocean Engineering*, **6** (1979) 593–615.
35. Li, Y. & Kareem, A., Computation of wave-induced drift forces introduced by displaced position of compliant offshore platforms. *Journal of Offshore Mechanics and Arctic Engineering, ASME*, **114** (1992) 175–184.
36. Li, Y. & Kareem, A., Parametric modelling of stochastic wave effects on offshore platforms. *Applied Ocean Research*, **15** (1993) 63–83.
37. Li, Y. & Kareem, A., Multivariate Hermite expansion of hydrodynamic drag loads on tension leg platforms. *Journal of Engineering Mechanics, ASCE*, **119**(1) (1993) 91 112.
38. Kareem, A. & Li, Y., Wind-excited surge response of a tension leg platform. *Journal of Engineering Mechanics, ASCE*, **119**(1) (1993) 161–183.
39. Kareem, A. & Li, Y., Stochastic response of tension leg platforms to viscous and potential drift forces. *Probabilistic Engineering Mechanics*, **9**(1) (1994) 1–14.
40. Winterstein, S. R., Ude, T. C. & Marthinsen, T., Volterra models of ocean structures: Extreme and fatigue reliability. *Journal of Engineering Mechanics, ASCE*, **120**(6) (1994) 1369–1385.
41. Kareem, A., Williams, A. N. & Hsieh, C. C., Diffraction of nonlinear random waves by a vertical cylinder in deep water. *Ocean Engineering*, **21**(2) (1994) 129–154.
42. Cochran, J. A., *The Analysis of Linear Integral Equations*. McGraw-Hill, New York, 1972.
43. Neal, E., The statistical distribution of second-order slowly varying forces and motions. *Applied Ocean Research*, **8**(2) (1972).
44. Vinje, T., On the statistical distribution of second-order forces and motions. *International Shipbuilding Progress*, **30** (1983) 58–68.
45. Naess, A., Statistical analysis of second-order response of marine structures. *Journal of Ship Research*, **29**(4) (1985) 270–284.
46. Langley, R. S. & McWilliams, S., A statistical analysis of first- and second-order vessel motions induced by waves and wind gusts. *Applied Ocean Research*, **15** (1993) 13–23.
47. Pugachev, V. S., *Probability Theory and Mathematical Statistics for Engineers*. Pergamon Press, Oxford, 1984.
48. Shinozuka, M. & Jan, C-M., Digital simulation of random processes and its applications. *Journal of Sound and Vibration*, **25**(1) (1972) 111–128.
49. Li, Y. & Kareem, A., Simulation of multivariate random processes: Hybrid DFT and digital filtering approach. *Journal of Engineering Mechanics, ASCE*, **119**(5) (1993) 1078–1098.
50. Ochi, M. K., Non-Gaussian random processes in ocean engineering. *Probabilistic Engineering Mechanics*, **1**(1) (1986) 28–39.
51. Grigoriu, M., Crossings of non-Gaussian translation processes. *Journal of Engineering Mechanics, ASCE*, **110**(4) (1984) 610–620.

APPENDIX A: PRESENT FORMULATION OF THE KAC–SIEGERT TECHNIQUE

The Fredholm homogeneous integral equation of the second kind is given by

$$\int_{-\infty}^{\infty} H_x^{(2)}(\omega_1, -\omega_2)\, G(\omega_1)\, G(\omega_2)\, \phi(\omega_2)\, \mathrm{d}\omega_2 = \lambda\phi(\omega_1), \tag{A.1}$$

where $G(\omega) = \sqrt{D(\omega)}$, and $D(\omega)$ is a two-sided spectrum. The discrete form of eqn (A.1) for N frequency points can be written as,

$$\sum_{j=1}^{N} G(\omega_i)\, H_x^{(2)}(\omega_i, -\omega_j)\, G(\omega_j)\, \phi(\omega_j)\, W_j \Delta + \sum_{j=1}^{N} G(\omega_i)\, H_x^{(2)}(\omega_i, \omega_j)\, G(\omega_j)\, \phi^*(\omega_j)\, W_j \Delta = \lambda\phi(\omega_i), \tag{A.2}$$

where the mesh interval, Δ, is constant for simplicity and an integration weighting factor, W_j, is included for improved accuracy.

We thus have a linear eigenvalue problem of dimension N which is expressible in matrix form as,

$$[A][W]\{\phi\} + [B][W]\{\phi\}^* = \lambda\{\phi\}, \tag{A.3}$$

where

$$A_{ij} = G(\omega_i)\, H_x^{(2)}(\omega_i, -\omega_j)\, G(\omega_j)\, \Delta,$$
$$B_{ij} = G(\omega_i)\, H_x^{(2)}(\omega_i, \omega_j)\, G(\omega_j)\, \Delta, \tag{A.4}$$

and $[W]$ is a diagonal matrix, whose elements are determined by the numerical integration method chosen. As an example, the weighting factor elements for the composite Simpson's rule are,

$$W_{1,1} = \tfrac{1}{3},\ W_{2,2} = \tfrac{4}{3},\ W_{3,3} = \tfrac{2}{3}, \ldots, W_{N-2,N-2} = \tfrac{2}{3},$$
$$W_{N-1,N-1} = \tfrac{4}{3},\ W_{N,N} = \tfrac{1}{3}.$$

Noting that eqn (A.3) is not Hermitian due to the involvement of the matrix of weighting factors, we introduce another diagonal matrix $[V]$, where $V_{i,i} = \sqrt{W_{i,i}}$. Then, a new vector may be specified as,

$$\{\Phi\} = [V]\{\varphi\}. \tag{A.5}$$

Multiplying both sides of (A.3) by $[V]$ leaves,

$$[V][A][V]\{\Phi\} + [V][B][V]\{\Phi\}^* = \lambda\{\Phi\}. \tag{A.6}$$

To solve eqn (A.6), we begin by rewriting $[A]$, $[B]$, and $\{\Phi\}$ in terms of their real and imaginary parts, i.e.

$$[A] = [A_R] + i[A_I],$$
$$[B] = [B_R] + i[B_I], \text{ and}$$
$$\{\Phi\} = \{\Phi_R\} + i\{\Phi_I\}.$$

Then the real matrix form which is equivalent to eqn

(A.6) is expressible as,

$$\begin{bmatrix} [V][A_R + B_R][V] & [V][B_I - A_I][V] \\ [V][A_I + B_I][V] & [V][A_R - B_R][V] \end{bmatrix} \begin{bmatrix} \Phi_R \\ \Phi_I \end{bmatrix} = \lambda \begin{bmatrix} \Phi_R \\ \Phi_I \end{bmatrix}. \tag{A.7}$$

which is symmetric when $[A_R]$, $[B_R]$, and $[B_I]$ are symmetric and $[A_I]^T = -[A_I]$.

Solving eqn (A.7) yields $2N$ real eigenvalues and $2N$ eigenvectors. Then, normalizing the eigenvectors and recombining the complex vectors, we have,

$$\{\phi\} = [V]^{-1}\{\Phi\} = [V]^{-1}\{\Phi_R + i\Phi_I\}. \tag{A.8}$$

According to the work by Kac and Siegert,[22] the nth-order cumulant, k_n, is obtained from,

$$k_n = \sum_{i=1}^{N} \left(\frac{n!}{2} \rho_i^2 \lambda_i^{n-2} (1 - \delta_{n1}) + \frac{(n-1)!}{2} \lambda_i^n \right), \tag{A.9}$$

where ρ_i is the first-order system coefficient, given by

$$\rho_i = \sum_{i=1}^{N} H_x^{(1)}(\omega_j) G(\omega_j) \phi_i^*(\omega_j) W_j \Delta. \tag{A.10}$$

APPENDIX B: PROBABILITY DENSITY AND CROSSING RATE APPROXIMATION METHODS

Gram–Charlier series distribution. This method is based on expanding the distribution of a non-Gaussian random variable, x, in a Hermite series with a Gaussian 'parent function.' The simplest form of this method is expressible as (e.g. Ref. 50)

$$p_G(x) = \frac{1}{\sqrt{2\pi}\sigma} \exp\left[-\frac{(x - m_1)^2}{2\sigma^2} \right] \times \left\{ 1 + \frac{\gamma_3}{3!} H_3\left(\frac{x - m_1}{\sigma}\right) + \frac{\gamma_4}{4!} H_4\left(\frac{x - m_1}{\sigma}\right) + \ldots \right\}. \tag{B.1}$$

The Gram–Charlier series distribution, however, has an inherent shortcoming in its limited ability to characterize the tail regions of the distribution and, thus, the extremes of a given process. In fact, this type of series expansion can exhibit negative probabilities in the tail regions.

Moment-based Hermite transformation methods. In this method, the non-Gaussian variable is expanded in Hermite polynomials in terms of a standardized Gaussian process.[23,51] This transformation is valid for a non-normal process, $x(t)$, which is expressible as a monotonic function of a standard normal process, $u(t)$. Having made this transformation, the probability density function of x may be derived as,

$$p_H(x) = \frac{1}{\sqrt{2\pi}} \exp\left[-\frac{u^2(x)}{2} \right] \frac{du(x)}{dx}. \tag{B.2}$$

Maximum entropy methods. In statistical mechanics, the entropy of a given state is directly related to its probability of occurrence. According to the principle of maximum entropy in one dimension, an appropriate probability density function, $p(x)$, must maximize the entropy functional,

$$H = -\int p(x) \ln p(x)\, dx, \tag{B.3}$$

while satisfying constraints specified via moment equations or moment values. Applying the constraints, in the present case the moment values themselves from our Volterra system analysis, via the Lagrange multiplier technique of variational calculus, the maximum entropy distribution is expressible as,

$$p_M(x) = \exp\left(-\sum_{k=0}^{N} \lambda_k x^k \right), \tag{B.4}$$

where N is the number of moments given and the coefficients (Lagrange multipliers) may be determined by matching the moments according to,

$$\int_{\infty}^{-\infty} x^n p_M(x)\, dx = m_n, \qquad n = 0, 1, \ldots, N. \tag{B.5}$$

and solving iteratively for the Lagrange multipliers. It has been noted, in addition, that since this system is highly nonlinear, the determination of these unknown coefficients or Lagrange multipliers is sensitive to the initial values chosen.[19] A discussion of an efficient scheme for determining the starting values for the λ_i is given in Ref. 19.

Mean upcrossing rate and distribution of maxima

The distribution of the maxima of a process can be approximated in terms of its mean upcrossing rate. Mathematically, the mean upcrossing rate is,

$$\nu(x) = \int_0^{\infty} \dot{x} p_{x,\dot{x}}(x, \dot{x})\, d\dot{x}. \tag{B.6}$$

This expression involves the joint probability density function of a random process and its first time derivative, which is difficult to obtain for an arbitrary non-Gaussian process. However, the crossing rate may be easily derived from the crossings of nonlinear transformations of Gaussian processes.[51] In the case of a moment-based Hermite transformation as described above wherein a non-Gaussian process, $x(t)$, is related to a Gaussian process, $u(t)$, the crossing rate may be written as,

$$\nu(x) = \nu_0 \exp\left(\frac{-u^2(x)}{2}\right), \tag{B.7}$$

where ν_0 is the zero-crossing rate given by $\sigma_u/2\pi$. The variance of the velocity of the parent Gaussian process is expressible in terms of the variances of the non-Gaussian process and its velocity.

An approximate distribution of the maxima of a non-Gaussian response may also be obtained using the Hermite method as,

$$p_E(x) = u(x) \exp\left(-\frac{u^2(x)}{2}\right) \frac{du(x)}{dx}. \tag{B.8}$$

For more detail, the reader is referred to Ref. 32.

APPENDIX C: CALCULATION OF EXPECTED VALUES FOR QUADRATIZATION OF WAVE FORCE

Here we will illustrate the computation of the expected values appearing in the right-hand side vector of eqn (35). Letting $v = u - \dot{x}_1$, v is a zero-mean Gaussian process with standard deviation, σ. The probability density function of v is thus,

$$f_V(v) = \frac{1}{\sqrt{2\pi}\sigma} \exp\left(-\frac{v^2}{2\sigma^2}\right). \tag{C.1}$$

Proceeding, then, we wish to first compute,

$$E[|v+U|(v+U)] = \int_{-\infty}^{\infty} |v+U|(v+U)\frac{1}{\sqrt{2\pi}\sigma} \times \exp\left(-\frac{v^2}{2\sigma^2}\right)dv = \int_{-U}^{\infty}(v+U)^2\frac{1}{\sqrt{2\pi}\sigma} \times \exp\left(-\frac{v^2}{2\sigma^2}\right)dv + \int_{-U}^{-\infty}(v+U)^2\frac{1}{\sqrt{2\pi}\sigma} \times \exp\left(-\frac{v^2}{2\sigma^2}\right)dv. \tag{C.2}$$

Expanding the polynomial in v and employing the properties of the even and odd functions in the expansion, we are left with

$$E[|v+U|(v+U)] = 2U^2\int_0^U \frac{1}{\sqrt{2\pi}\sigma}\exp\left(-\frac{v^2}{2\sigma^2}\right)dv + \frac{4U\sigma}{\sqrt{2\pi}}\exp\left(-\frac{U^2}{2\sigma^2}\right) + \int_0^U v^2\frac{1}{\sqrt{2\pi}\sigma}\exp\left(-\frac{v^2}{2\sigma^2}\right)dv.$$

Letting $y = v/\sigma$, and integrating the last term above by parts, we have finally,

$$E[|v+U|(v+U)] = 2(U^2+\sigma^2)\int_0^{U/\sigma}\frac{1}{\sqrt{2\pi}} \times \exp\left(-\frac{y^2}{2}\right)dy + \frac{2U\sigma}{\sqrt{2\pi}}\exp\left(-\frac{U^2}{2\sigma^2}\right). \tag{C.3}$$

Next, we will compute,

$$E[v|v+U|(v+U)] = \int_{-\infty}^{\infty} v|v+U|(v+U)\frac{1}{\sqrt{2\pi}\sigma} \times \exp\left(-\frac{v^2}{2\sigma^2}\right)dv = \int_{-U}^{\infty} v(v+U)^2\frac{1}{\sqrt{2\pi}\sigma} \times \exp\left(-\frac{v^2}{2\sigma^2}\right)dv + \int_{-U}^{-\infty} v(v+U)^2\frac{1}{\sqrt{2\pi}\sigma} \times \exp\left(-\frac{v^2}{2\sigma^2}\right)dv. \tag{C.4}$$

Again, expanding the polynomial in v and employing even and odd function properties, we have,

$$E[v|v+U|(v+U)] = \frac{2U^2\sigma}{\sqrt{2\pi}}\exp\left(-\frac{U^2}{2\sigma^2}\right) + 2\int_U^{\infty} v^3\frac{1}{\sqrt{2\pi}\sigma}\exp\left(-\frac{v^2}{2\sigma^2}\right)dv + 4\int_0^U Uv^2\frac{1}{\sqrt{2\pi}\sigma}\exp\left(-\frac{v^2}{2\sigma^2}\right)dv.$$

Integrating the latter two terms by parts yields,

$$E[v|v+U|(v+U)] = 4U\sigma^2\int_0^{U/\sigma}\frac{1}{\sqrt{2\pi}} \times \exp\left(-\frac{y^2}{2}\right)dy + \frac{4\sigma^3}{\sqrt{2\pi}}\exp\left(-\frac{U^2}{2\sigma^2}\right). \tag{C.5}$$

Finally, we wish to compute

$$E[v^2|v+U|(v+U)] = \int_{-\infty}^{\infty} v^2|v+U|(v+U) \times \frac{1}{\sqrt{2\pi}\sigma}\exp\left(-\frac{v^2}{2\sigma^2}\right)dv = \int_{-U}^{\infty} v^2(v+U)^2 \times \frac{1}{\sqrt{2\pi}\sigma}\exp\left(-\frac{v^2}{2\sigma^2}\right)dv + \int_{-U}^{-\infty} v^2(v+U)^2 \times \frac{1}{\sqrt{2\pi}\sigma}\exp\left(-\frac{v^2}{2\sigma^2}\right)dv. \tag{C.6}$$

Following the same procedure as laid out previously, multiplying out the polynomial in v and taking advantage of the even or odd character of each term in the expansion, we have,

$$E[v^2|v+U|(v+U)] = 2\int_0^U v^4 \frac{1}{\sqrt{2\pi}\sigma} \times \exp\left(-\frac{v^2}{2\sigma^2}\right) dv + 2U^2 \int_0^U v^2 \frac{1}{\sqrt{2\pi}\sigma} \times \exp\left(-\frac{v^2}{2\sigma^2}\right) dv + 4U \int_U^\infty v^3 \frac{1}{\sqrt{2\pi}\sigma} \times \exp\left(-\frac{v^2}{2\sigma^2}\right) dv.$$

Integrating each of the terms above by parts one or more times, we are left with

$$E[v^2|v+U|(v+U)] = 2\sigma^2(U^2+3\sigma^2)\int_0^{U/\sigma} \frac{1}{\sqrt{2\pi}} \times \exp\left(-\frac{y^2}{2}\right) dy + \frac{2U\sigma^3}{\sqrt{2\pi}} \exp\left(-\frac{U^2}{2\sigma^2}\right). \quad \text{(C.7)}$$